On spiral glider-guns in hexagonal cellular automata: activator-inhibitor paradigm

Andrew Wuensche[1], **Andrew Adamatzky**[2]

[1]Discrete Dynamics Lab (www.ddlab.org), UK
andy@ddlab.org
[2]Faculty of Computing, Engineering and Mathematical Sciences, University of the West of England, Bristol BS16 1QY, UK
andrew.adamatzky@uwe.ac.uk

Pre-Print: Nov 2005

Abstract

We present a cellular-automaton model of a reaction-diffusion excitable system with concentration dependent inhibition of the activator, and study the dynamics of mobile localizations (gliders) and their generators. We analyze a three-state totalistic cellular automaton on a two-dimensional lattice with hexagonal tiling, where each cell connects with 6 others. We show that a set of specific rules support spiral glider-guns (rotating activator-inhibitor spirals emitting mobile localizations) and stationary localizations which destroy or modify gliders, along with a rich diversity of emergent structures with computational properties. We describe how structures are created and annihilated by glider collisions, and begin to explore the necessary processes that generate this kind of complex dynamics.

keywords: cellular automata, reaction-diffusion, glider, glider-gun, localization, emergence, complexity, mutation, self-organization, dynamics.

1 Introduction

Two-dimensional cellular automata (CA), with three (or more) cell-states have a propensity for generating complex dynamics, comprising emergent interacting structures with computational properties[19, 3]. There is a heightened probability of finding complex rules in three-state (ternary) rule-space than in binary rule-space. This is not surprising as at least three states are required for reaction-diffusion interactions to be included, an interpretation which would be difficult to apply to the legendary Game-of-Life, the best example of complexity in binary 2D CA (which we do not intend to re-examine here). Rather, we wish to explore and understand the many possibilities for complex dynamics in ternary cell-state rule spaces.

Cellular-automaton models of chemical systems and excitation dynamics have proved to be effective tools for studying complex spatio-temporal phenomena in active non-linear systems[15, 12, 16, 10] and fast-prototyping reaction-diffusion computing devices[1]. Of particular interest are models of reaction-diffusion media which exhibit traveling localizations of compact patterns in their dynamics, known as gliders in cellular-automaton theory. In the framework of collision-based computing[2] the traveling localizations are used to represent quanta of information, and to perform computation by implementing basic logical gates when they collide or interact.

Despite the sophisticated level of development of cellular-automaton models of collision-based computing in reaction-diffusion systems, a notable drawback has been the absence of stationary generators of mobile localizations, analogs of glider-guns in the game-of-life, which are invaluable structures for implementing constant logical truth and subsequent negation, to achieve functionally complete logical systems.

In this paper we present a breakthrough in the field — the discovery of reaction-diffusion transition rules which support the existence of stationary generators of mobile patterns (glider-guns), and stationary localizations which interact with gliders. A snapshot of the dynamics is shown in Fig.1.

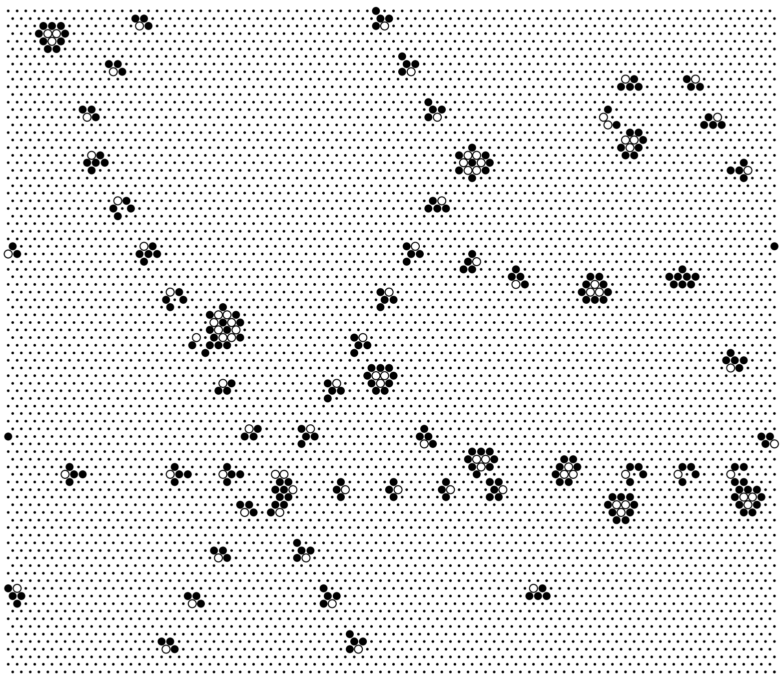

Figure 1: A snapshot of the 7-neighbor spiral rule on a hexagonal lattice 88×88, with periodic (toroidal) boundaries. The 3 cell-states [0,1,2] are indicated by [$\cdot$ $\circ$ $\bullet$]. Emergent structures include two types of spiral glider-guns, and two types of stationary localizations which destroy or modify small gliders. The dynamics seen here have settled from a random initial configuration with an approximately equal density of 2s, 1s and 0s.

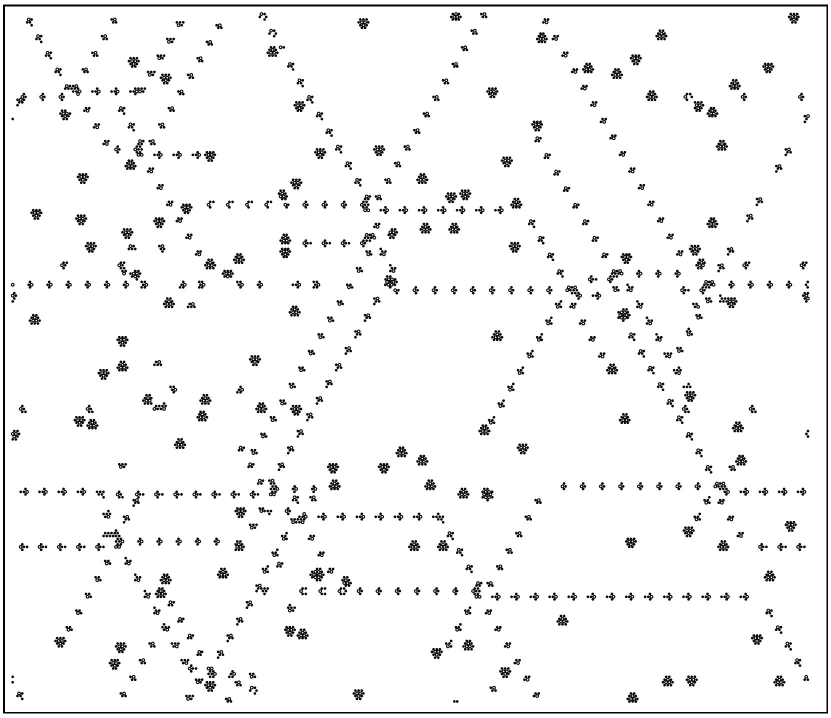

Figure 2: A snapshot of the spiral rule on a 250 × 250 hexagonal lattice, which has evolved over 550 time-steps. Quasi-stable circuits have emerged from interacting glider-guns and stationary localizations. The initial configuration was random with an approximately equal density of 2s, 1s and 0s.

We will confine our investigation to totalistic CA[8, 19], where a cell's update depends on just the number of different cell-states in its neighborhood, and also to just three cell-states (2, 1 and 0), which can also be understood as cell-colors or cell-values[19].

The overwhelming majority of CA rules with a neighborhood size $k > 3$ exhibit chaotic behavior[17, 19], but there are automatic methods for categorizing rule-space to find the relatively rare complex rules[17, 19]. Ternary rules supporting 2D glider dynamics, both on square and hexagonal tilings, have been found by these methods[19], with neighborhood sizes from 4 to 9, most notably the 6-neighbor hexagonal "beehive" rule[19]. This was later shown to implement collision-based logical universality based on the reaction-diffusion analysis of its behavior[3]. The emergent structures in the beehive rule include gliders (mobile localizations), self-reproduction by glider collisions, polymer-like gliders, mobile glider-guns, and a somewhat elusive spiral glider-gun[18], but no stationary localizations.

In this paper we introduce the 7-neighbor "spiral" rule (and its variants), where the neighborhood consists of the central cell and its six nearest neighbors on a two-dimensional lattice with hexagonal tiling. The dynamics display all of the same kind of the emergent structures found in the beehive rule, but also two additional kinds of structure: "stationary" spiral glider-guns (i.e. rooted in a fixed position), and stationary localizations which destroy or modify gliders. These structures emerge readily in the system's evolution from random initial patterns, or from subsequent collisions and interactions between small gliders and other structures.

The spiral rule derives its name from the fact that a glider-gun's central generator rotates, causing ejected gliders to form a growing spiral, behaving like the tips of spiral wave fragments in excitable chemical media.

There are two types of spiral glider-guns, shooting gliders in six directions, which can even combine into more complex glider-guns. Any of these glider streams can be blocked (or modified) by stationary localizations to create a variety of flexible stationary glider-guns, a key ingredient in glider-based computation. Once formed, spiral glider-guns and stationary localizations are relatively stable (though not immune) from attack by other gliders, and tend to form large scale quasi-stable circuits as in Fig. 2, which also displays many kinds of lower level interactions and rhymes.

The spiral rule resides within a family of related rules. We begin to explore the necessary processes that allow the structures to emerge in the hope of finding an underlying principle of self-organization.

2 Building the rules

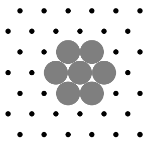

Figure 3: The $k = 7$ neighborhood on a 2D hexagonal lattice. The central cell updates its state according to the frequency of different states in its neighborhood, including itself.

The transition rules studied here are totalistic rules, a subset of cellular automata rule-space. In a totalistic rule (also called a k-totalistic rule[8]) a cell updates its state depending just on the totals of different cell-states in its neighborhood (Fig. 3), irrespective of cell-state positions, so the dynamics conserve symmetry, and are neutral to orientation or spin direction. For ternary CA ($k = 3$) the update rule can be written as follows: $x^{t+1} = f(\sigma_2(x)^t, \sigma_1(x)^t, \sigma_0(x)^t)$, where $\sigma_s(x)^t$ is the number of cell x's neighbors with cell-state $s \in \{2, 1, 0\}$ at time step t. As for all classical CA, cell updates are made synchronously across the whole lattice in discrete time-steps.

A rule can be expressed as a lookup table whose output-states make up a rule-table (Fig. 4). For a cellular automaton with $v = 3$ cell-states and neighborhood size $k = 7$, the rule-table is constructed as follows: an output (2, 1 or 0)

```
        rule-table index
       /  totals: 2s+1s+0s=k=7
      /  /         rule-table
     /  /         / mutations
    / 2_1_0     /  2___1___0
 0: 0 0 7 : 0 > o   c   .
 1: 0 1 6 : 1 > o   .   o
 2: 0 2 5 : 2   .   g   g
 3: 0 3 4 : 1 + G   .   G
 4: 0 4 3 : 2 - .   G   G
 5: 0 5 2 : 2 - .   G   G
 6: 0 6 1 : 2 + .   G   G
 7: 0 7 0 : 2 + .   G   G
 8: 1 0 6 : 0 > o   c   .
 9: 1 1 5 : 2 > .   c   c
10: 1 2 4 : 2   .   G   g
11: 1 3 3 : 1 + G   .   G
12: 1 4 2 : 2 + .   G   G
13: 1 5 1 : 2 + .   G   G
14: 1 6 0 : 2 + .   G   G
15: 2 0 5 : 0 > c   c   .
16: 2 1 4 : 0 > o   c   .
17: 2 2 3 : 2   .   c   g
18: 2 3 2 : 1 - G   .   G
19: 2 4 1 : 2 + .   G   G
20: 2 5 0 : 2 + .   G   G
21: 3 0 4 : 0 > g   c   .
22: 3 1 3 : 2 > .   c   g
23: 3 2 2 : 2   .   g   g
24: 3 3 1 : 1   g   .   g
25: 3 4 0 : 2 - .   G   G
26: 4 0 3 : 0   g   G   .
27: 4 1 2 : 0 > G   c   .
28: 4 2 1 : 2   .   cg  g
29: 4 3 0 : 1   g   .   g
30: 5 0 2 : 0   G   c   .
31: 5 1 1 : 0 > G   c   .
32: 5 2 0 : 2 - .   G   G
33: 6 0 1 : 0   G   c   .
34: 6 1 0 : 0   G   cg  .
35: 7 0 0 : 0 - G   G   .
```

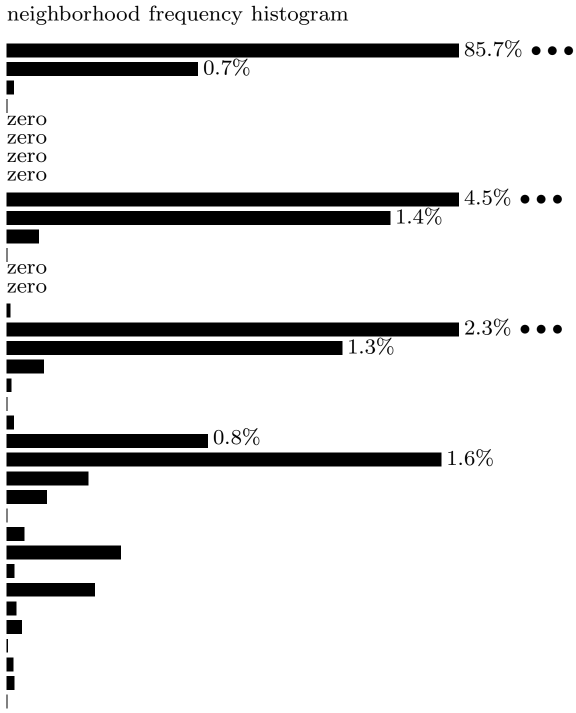

Figure 4: The look-up table of a $[v,k]=[3,7]$ totalistic rule has 36 entries. The neighborhood index (0 to 35), the cell-state totals (which must add up to $k=7$), and the rule outputs of the spiral rule, are tabulated on the left (for example, 22: 3 1 3 : 2). In the center, the results of all 72 possible single cell-state mutations are summarized (two mutations for each entry). The symbols **G**, **g**, **c** and **o** signify the following behavior in relation to mutations, **G**: the mutation is quasi-neutral, **g**: slightly different glider dynamics emerge, **c**: the dynamics becomes chaotic, **cg**: the dynamics tend to chaos but with gliders present, **o**: the dynamics results in order (a point attractor). 15 neighborhoods can be regarded as wildcards, making no impact, or minimal impact, on the dynamics, designated by "+" strong wildcards, and "−" weak wildcards. 10 neighborhoods are essential for glider dynamics, indicated by ">". The wildcard and glider neighborhoods correlate well with the neighborhood-frequency histogram shown on the right.

is assigned to each of the 36 possible frequencies of the three states in the $k=7$ neighborhood. If the three totals in the order [2s, 1s, 0s] are taken as a decimal number, then the rule-table follows a descending order of these numbers, with 700 (index 35) on the left and 007 (index 0) on the right. Note that the total of 0s can be omitted as it follows from the totals of 2s and 1s. The rule-table of the spiral rule in this paper is: 0002001200212202212002221220222221210.

We have mutated the rule-table by flipping each output separately to the two possible alternatives, and observed the resulting dynamics with DDLab[18]. The results are summarized in Fig. 4. Of all 72 possible single cell-state mutations, 36 are quasi-neutral, i.e. do not cause dramatic changes in the space-time dynamics of the spiral rule cellular automaton. See the DDLab website[18] link to the "spiral-rule" for snapshots of all 72 mutants. Fifteen neighborhoods are identified as wildcards, meaning that their outputs could be assigned at random with minimal impact on the dynamics. There are 9 strong wildcards (marked with "+") which make no significant impact, and 6 weak wildcards (marked with "−") which make some difference to the details of interactions, but not to the main features — gliders, glider-guns, and stationary localizations. This correlates closely with the neighborhood-frequency histogram[17] (also known as the input-frequency histogram) on the right in Fig. 4, which shows the probability of the neighborhoods occurring in the evolved system in Fig. 1, taken over 1000 time steps.

Examining the integrity and motion of the five basic gliders (Fig. 6), ten neighborhoods (and their outputs) are found to be essential, indicated by ">". This also correlates with the neighborhood frequency histogram, which shows a high probability of these neighborhoods occurring.

To summarize, the rule-table in Fig. 4 (and its matrix version in Fig. 5c), indicates which outputs are essential, and which are quasi-neutral, having little or no effect on the dynamics — they could be wild-cards. The results were deduced experimentally by firstly testing all possible mutations with DDLab[18], and secondly by measuring the neighborhood frequency[17] in an evolved system, shown as a histogram in Fig. 4. A very low or zero frequency indicates neighborhoods whose survival would be unlikely, or impossible, in an evolved system not subject to noise (i.e. deterministic), so their outputs would be neutral to mutation. Lastly, the critical outputs that play a role in generating gliders and other structures can be identified by looking at the localization logic involved, for example in glider motion and stationary localization stability.

3 Reaction-Diffusion Interpretation

One of the paper's aims was to explore further possible designs of collision-based chemical computers, non-classical computing architectures where information is transferred by mobile localizations, e.g. wave-fragments in a sub-excitable Belousov-Zhabotinsky (BZ) medium, and where computation is implemented in collisions of the mobile localizations[1]. Cellular automata are computationally fast prototypes of reaction-diffusion computers, the models include BZ reactions[6], chemical systems exhibiting Turing patterns[23, 20, 22], precipitating systems[1], calcium wave dynamics[21], and chemical turbulence[7].

Therefore we consider it reasonable to provide an interpretation of the rules we have discovered in terms of reaction-diffusion chemical systems, which we envisage will provide the basis for experimental chemical laboratory designs of reaction-diffusion computers, allowing stationary localizations to be used as memory units[2].

i \ j	0	1	2	3	4	5	6	7
0	0	1	2	1	0	0	0	0
1	0	2	2	1	0	0	0	
2	0	0	2	1	0	0		
3	0	0	2	1	0			
4	0	0	2	1				
5	0	0	2					
6	0	0						
7	0							

(a) rule M_1

i \ j	0	1	2	3	4	5	6	7
0	0	1	2	1	2	2	2	2
1	0	2	2	1	2	2	2	
2	0	0	2	1	2	2		
3	0	0	2	1	2			
4	0	0	2	1				
5	0	0	2					
6	0	0						
7	0							

(b) rule M_2

i \ j	0	1	2	3	4	5	6	7
0	0	1	2	1	2	2	2	2
1	0	2	2	1	2	2	2	
2	0	0	2	1	2	2		
3	0	2	2	1	2			
4	0	0	2	1				
5	0	0	2					
6	0	0						
7	0							

(c) rule M_3

i \ j	0	1	2	3	4	5	6	7
0	0	1	2	+	−	−	+	+
1	0	2	2	+	+	+	+	
2	0	0	2	−	+	+		
3	0	2	2	1	−			
4	0	0	2	1				
5	0	0	−					
6	0	0						
7	−							

(d) rule M_*

Figure 5: The transition matrix representations of spiral rules. Rules (a) and (b) permit the existence of spiral glider-guns, while rule (c), the spiral rule, also exhibits stationary localizations. Rule (d) is the spiral rule with wild-cards, where the output makes little ("−") or no ("+") difference to the evolved, settled, dynamics.

We adopt an alternative formalism[3], where the rule-table in Fig. 4 is represented as a state transition matrix in Fig. 5, defined as follows: the state of each neighborhood is described by the row-index i (the number of neighbors in cell-state 2) and column-index j (the number of neighbors in cell-state 1). We do not have to count the number of neighbors in cell-state 0, because it is given by $7-(i+j)$. A cell with a neighborhood represented by indices i and j will update to cell-state $M[i][j]$ which can be read off the matrix. In terms of the cell-state transition function this can be presented as follows: $x^{t+1} = M[\sigma_2(x)^t][\sigma_1(x)^t]$.

To derive sets of chemical reactions which experimental chemists would recognize, we interpret the cell-state as follows: '1' is the activator A, '2' is the inhibitor I, and '0' is the substrate S. Then the transition matrix (Fig. 5) represents an abstract chemical reaction as follows: $i + j \rightarrow M[i][j]$.

Thus, the simplest transition matrix M_1 in Fig. 5a provides us with a number of hints to understand the equivalent abstract chemical reactions. $M_1[0][1] = 1$

symbolizes the diffusion of the activator; if a 'molecule' of activator is present in the vicinity of the medium's micro-volume filled with the substrate, the activator diffuses into the micro-volume. $M_1[1][1] = 2$ symbolizes the suppression of the activator by the inhibitor; a micro-volume occupied by the activator changes into the inhibitor. Similarly, $M_1[i][2] = 2$ $(i = 0, \cdots, 5)$ can be interpreted as the self-inhibition of the activator in particular concentrations. $M_1[i][3] = 1$ $(i = 0, \cdots, 4)$ symbolizes a sustained excitation under particular concentrations of the activator. Finally, $M_1[i][0] = 0$ $(i = 1, \cdots, 7)$ means that the inhibitor is dissociated in the absence of the activator to produce the substrate, and that the activator does not diffuse in sub-threshold concentrations. The complete set of quasi-chemical reactions between activator A, inhibitor I and substrate S looks as follows:

$$
\begin{aligned}
&A + 6S \rightarrow A \\
&A + I \rightarrow I \\
&2A \rightarrow I \\
&3A \rightarrow A \\
&I \rightarrow S.
\end{aligned}
$$

Other domains of matrix M_1 (Fig. 5a) determine the specific concentration-dependent diffusion of the activator and inhibitor. Let us consider the domains defined as $M_1[i][j] = 0$. Zero entries in the matrix indexed by $j \geq 4$ and $i = 1$ show that the diffusion of the inhibitor is limited by the inhibitor's concentration. Zero entries for $i \geq 4$ $(0 \leq j \leq 7)$ means that when the concentration of the activator exceeds a threshold of 4, the activator does not diffuse and no inhibitor is formed.

The matrix domain $M_1[i][j] = 0$ for $j \geq 4$ seems to contradict real-life experience[1] because an activator exceeding a certain concentration is likely to diffuse, not stay localized. To avoid this artifact we upgrade M_1 to a more "realistic" transition matrix M_2 (Fig. 5b). There $M_1[i][j] = 2$ for $j \geq 4$, which is interpreted as an upper-threshold of self-inhibition, where the threshold has value of 4:

$$
\begin{aligned}
&A + 6S \rightarrow A \\
&A + I \rightarrow I \\
&2A \rightarrow I \\
&3A \rightarrow A \\
&\beta A \rightarrow I (\beta \geq 4) \\
&I \rightarrow S.
\end{aligned}
$$

As mentioned before, the automata models governed by the rule matrices M_1 and M_2 form spiral glider-guns (even when starting their evolution from a random initial configuration), with the dynamics rapidly becoming rich in gliders. The gliders, which are analogs of traveling wave-fragments[1] or dissipative solitons[5], are essential components of collision-based reaction-diffusion computers[1]. However, no stationary localizations are produced in the automaton's evolution. The stationary localizations are necessary to implement optimal computing architectures – with basic memory units – in spatially-extended non-linear media[2]. So far, we are not aware of any published reports of chemical laboratory implementations of liquid-phase chemical systems, where mobile and stationary localizations coexist in the same reaction space. To encourage the development of such chemical media we can modify matrix M_2 to matrix M_3 (Fig. 5c) so that $M_3[3][1] = 2$:

$$\begin{array}{l} A + 6S \rightarrow A \\ A + I \rightarrow I \\ A + 3I \rightarrow I \\ A + 2I \rightarrow S \\ 2A \rightarrow I \\ 3A \rightarrow A \\ \beta A \rightarrow I \\ I \rightarrow S. \end{array}$$

The rule reflects the nonlinearity of activator-inhibitor interactions for sub-threshold concentrations of the activator. Namely, for a small concentration of the inhibitor ($i = 1$), and for inhibitor threshold concentrations ($i = 3$), the activator is suppressed by the inhibitor, while for critical concentrations of the inhibitor ($i = 2$) both the inhibitor and activator dissociate, producing the substrate.

4 Emergence of gliders and spiral glider-guns

The spiral-rule and its various precursors and mutations (in Figs. 4 and 5) exhibit an extremely rich diversity of space-time localization dynamics — gliders and their generators, together with stationary localizations. In the following sections of the paper we will illustrate and discuss the basic dynamics of the spiral-rule cellular automata itself.

Fig. 1 gives a snapshot of an evolved system from a random initial configuration on a 88×88 lattice. Emergent structures include two types of spiral glider-gun. A high-frequency gun (lower left), a low-frequency gun (upper right), and two types of stationary localizations which destroy or modify gliders. Gliders typically have a white head, (cell-state=1), a black black body and tail (cell-state=2), and move headfirst against a neutral background of dots (cell-state=0). Fig. 2 shows a larger lattice (250×250), where the dynamics has evolved over 550 time-steps from a random initial configuration. In both cases, quasi-stable circuits have emerged formed from interacting glider-guns and stationary localizations, but lower level interactions and rhythms continue.

The spiral glider-guns to some extent resemble the spiral waves commonly observed in simulations and laboratory experiments with excitable reaction-diffusion media. A spiral glider-gun has a rotating (and quasi-stationary) tip which spreads activation waves outward. However, in contrast to "conventional" spiral waves, the spreading wave-front is not uninterrupted but splits into several localized wave-fragments, gliders, unlike those observed in active chemical BZ systems in sub-excitable mode[14]. In these systems we have never observed a spiral breaking up into wave-fragments and at the same time preserve its rotating core (in constant experimental conditions), neither in simulated nor experimental BZ systems. There is, however, evidence of complete spiral breakup and subsequent transition to spatio-temporal chaotic states, e.g. reported in [13].

Phenomenology that is closest to spiral breakup in our cellular-automaton spiral glider-guns was studied numerically in [4]. There, a modified Barkley model of an excitation reaction-diffusion system was employed to demonstrate the break up of a spiral wave far away from the core, or rotating tip, of the spiral. However, this was achieved in somewhat "artificial" conditions, in which the ratio of time-scales, of the local dynamics of the activator and inhibitor variables, were dynamically changing, increasing during the course of numerical integration.

5 Gliders and their interactions

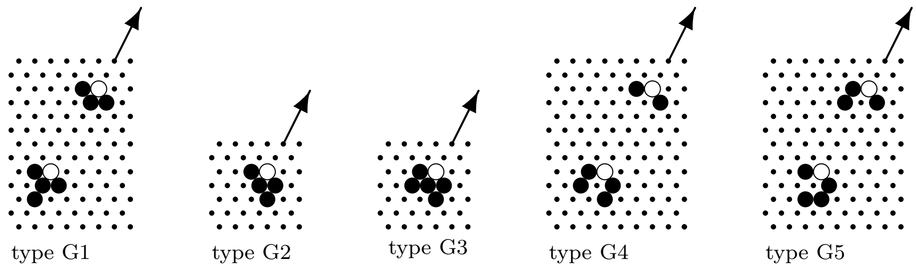

Figure 6: Five types of basic gliders (G1-G5), which have just one head, show moving NE. Types G2 and G3 have period one, types G1, G4 and G5 have period 2.

In the spiral-rule cellular automaton, each cell that forms a glider and its surroundings must change to the correct cell-state at the next time-step according to the rule-table outputs in Fig. 4. While mutations to some of these outputs disrupt the dynamics, a significant fraction of outputs are quasi-neutral. The most disruptive mutations belong to neighborhoods that play a crucial part in maintaining the integrity of the most common emergent localizations, the basic gliders, which is easily confirmed by analyzing glider motion. These neighborhoods are also the most frequently occurring in the evolved dynamics, while the frequency of quasi-neutral neighborhoods is very low or zero (Fig. 4).

Five types of basic gliders (which have just one head) were discovered in the spiral rule, shown in Fig. 6 (G1-G5). They have a 1-state head (white circle) and a (sometimes breathing) 2-state tail (black disc). Gliders move headfirst in any of the 12 possible directions on the hexagonal lattice. Types G2 and G3 have period one, types G1, G4 and G5 have period 2. Asymmetric gliders, types G2 and G5 can be handed. The high-frequency glider-gun shoots type G1 gliders, the low-frequency glider-gun shoots type G2 gliders (see Fig. 11).

Small two-headed gliders are present in the spiral rule, and just a few ex-

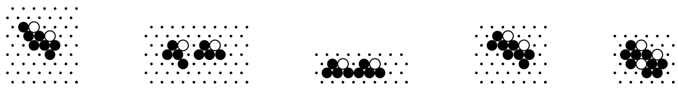

Figure 7: Just a few of the various types of small two headed gliders, all heading NE.

amples are shown in Fig. 7, all heading NE. Some of these two-headed gliders are basic single headed gliders that have combined, and we find that arbitrary length polymer gliders in many combinations can exist made up of aggregations of simpler gliders.

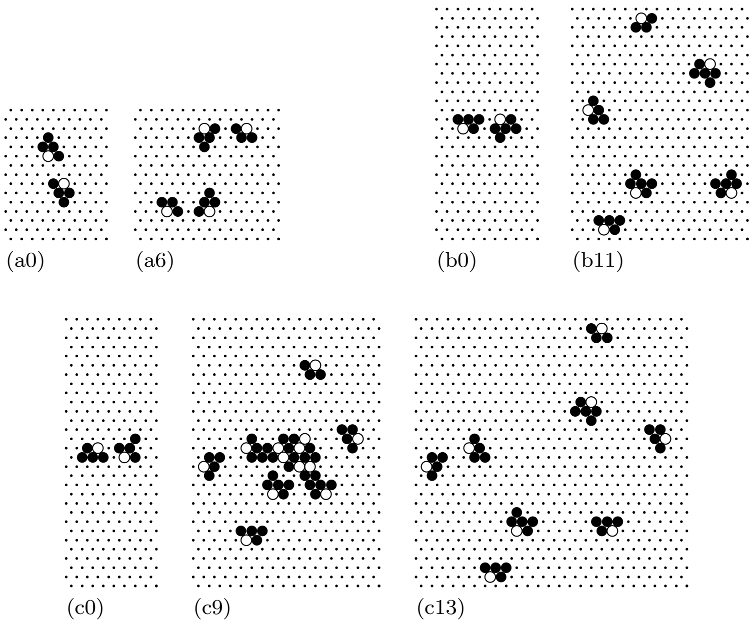

Figure 8: Glider reproduction by pairwise collisions between basic gliders. After a complicated transient interaction phase, gliders of different types emerge as follows: (a) 4 gliders after 6 time-steps, (b) 6 gliders after 11 time-steps, (c) 8 gliders after 13 time-steps, showing the transient interaction at time-step 9.

The outcomes of simple pairwise glider collisions are surprisingly rich, including conservation, destruction, modification, and reproduction. Collision outcomes depend on the exact point and direction of impact. More complex dynamics result from collisions between three or more gliders, and from repetitive interactions involving streams of gliders shot from glider-guns. Simple pairwise collisions between the beehive rule glider were fully explored in [19], but for the 5 types of gliders in the spiral rule just a few examples that lead to glider reproduction are shown in Fig. 8. After a collision there is typically a phase of transient interaction where a complicated pattern evolves over several time-steps before settling into a new set of emergent gliders. Gliders that collide with the interaction phase would further complicate potential outcomes.

In the example in Fig. 8a, glider G2 moving NE collides with G2 moving SW; after six time-steps four gliders emerge: 2 G2s and 2 G1s. In example 8b a G2 glider moving SW collides with G3 moving NW; after 11 time-steps 6 gliders emerge: one G1, 2 G2s and 3 G3s. An even more complicated scenario unfolds in example 8c yielding 8 gliders, when glider G2 moving NE collides with glider G1 moving SW. The intermediate phase at time-step 9 shows that 4 gliders have already detached themselves from a central transient area: one G1 and 3 G2s. By time-step 13 the central transient area has broken up into 4 more gliders: 2 G2s and 2 G3s.

6 Stationary localizations

There are two basic types of stationary localization, SL1 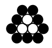 and SL2 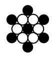 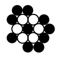, the later with a variable outer coating. Both interact with gliders, either to destroy or absorb gliders on impact, or to modify gliders that brush past — the snapshot in Fig. 1 includes both types.

For example, SL1 can change glider G1 to G2 and G2 to G1; it also takes part in constructing the low-frequency spiral glider-gun. SL2 can change G1 to G5, or G1 to alternating G3-G4. SL2 has a kind of memory, provided by its variable outer black coating of 2s (black cells). SL2 is stable with six black cells in a permanent outer coating equally spaced around the central hexagon, but six extra black cells can be deposited or removed in the gaps in the permanent coating, by passing gliders. This changes SL2's interactive properties with the next glider to come along, which can become a repetitive process when a glider stream brushes past SL2 localizations.

The two types of stationary localizations can link up in many combinations (of arbitrary size) to create chains, aggregations and oscillators; just a few are shown in Fig. 9.

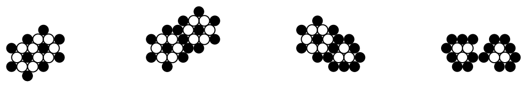

Figure 9: Examples of linked stationary localizations SL1 and SL2, forming chains, aggregations and oscillators. Many combinations of arbitrary size are possible.

Stationary localizations emerge in the evolution of the cellular automaton as a result of glider collisions and other interactions. In Fig. 10a we see a glider G2 moving East about to collide with a glider G5 moving NW, then an intermediate transient phase (Fig. 10b) at time-step 7. After 11 time-steps (Fig. 10c) the stationary localization SL1 has been created in the center, and 4 gliders have been ejected: 3 G2s and one G3.

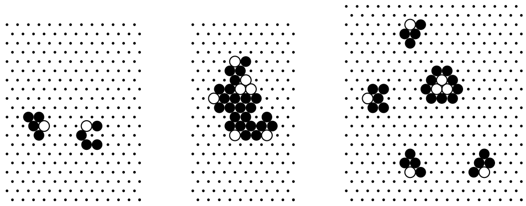

(a) step 0 (b) step 7 (c) step 11

Figure 10: Creating the stationary localization SL1 by a pairwise glider collision, which also produces 4 gliders.

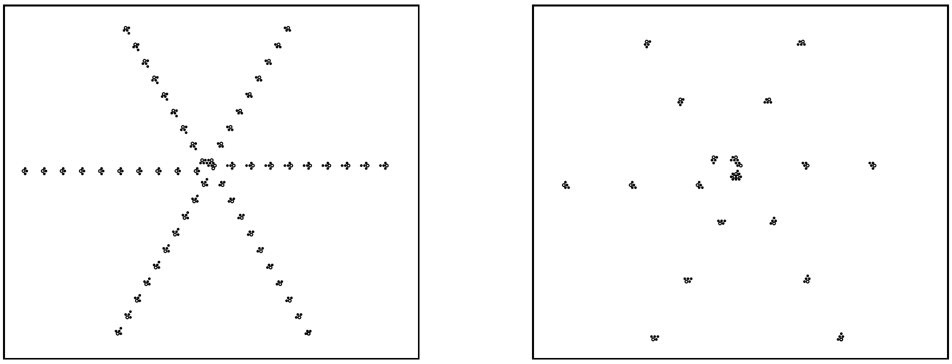

(a) (b)

Figure 11: (a) The high-frequency spiral glider-gun (SGG1), shooting G1 gliders spaced apart by 6 cells or time-steps. (b) The low-frequency spiral glider-gun (SGG2), shooting G2 gliders spaced apart by 21 cells or time-steps.

7 Spiral glider-guns

The spiral rule supports two types of spiral glider-gun, a high-frequency gun shooting G1 gliders (SGG1) shown in Fig. 11a, and a low-frequency glider gun shooting G2 gliders at a slower rate (SGG2) shown in Fig. 11b. The interval between successive gliders in the glider stream is 6 cells for high-frequency and 21 cells for low-frequency.

Both glider-guns shoot gliders in six directions, and can of course rotate both clockwise or anti-clockwise, following the symmetric properties of totalistic rules.

The spiral glider-guns emerge from random initial configurations. Remarkably, they can even combine to form compound glider-guns as in Fig. 12, where two spiral glider-guns have formed a complex central generator of glider streams: a high-frequency (SGG1) rotating clockwise, and low-frequency (SGG2) rotating anticlockwise, which is just above SGG1. This compound structure emerged spontaneously within a random initial configuration, and was then isolated.

We are interested to discover how the two types of spiral glider-gun might be generated by collisions between the "elementary particles" of the cellular automaton, the simple gliders and stationary localizations.

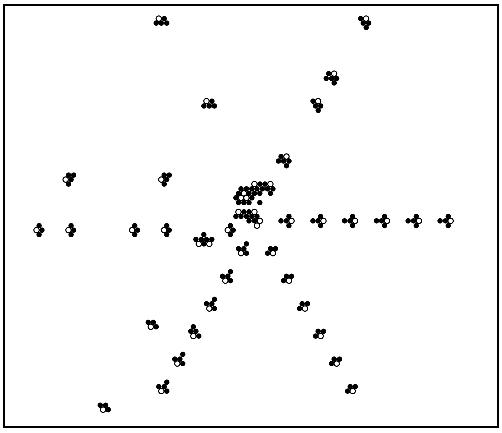

Figure 12: Two glider-guns combined into a complex central generator of glider streams: high-frequency (SGG1) rotating clockwise, and low-frequency (SGG2) rotating clockwise.

In a variation to the spiral rule[1], which has the same phenomenology except that the low-frequency glide-gun (SGG2) is absent, we had discovered a simple pairwise glider collision which generated the central core of the high-frequency glider-gun (SGG1) after eight time-steps. The collision is between a G2 glider moving East and a G5 moving NW pictured here: 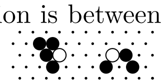 . However, the simplest generators of SGG1 found so far in the spiral-rule itself require colliding several gliders simultaneously into each other as shown in Figs. 13, although other generators based on particle collisions probably exist.

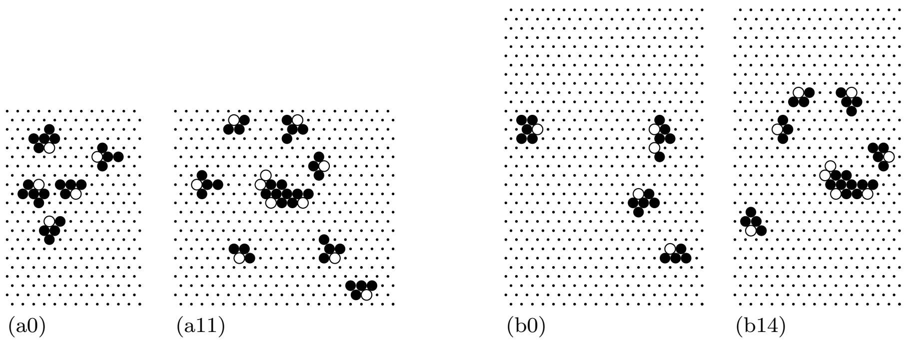

Figure 13: Two methods of creating a high-frequency spiral glider-gun (SGG1) by colliding "elementary particles": (a) with 5 basic gliders, (b) with 3 basic gliders and small 2-headed glider.

The first SGG1 generator consists of five basic gliders, which are shown about to collide (Fig. 13a0), 2 G2s heading SE and NW, 2 G3s heading SE and

[1] The spiral rule precursor's rule-table is 000002020000220002200011222000021210

NE, and a G1 heading East. By time-step 11 (Fig. 13a11) the central structure SGG1 has formed, rotating clockwise, and a glider belonging to each of the 6 G1 glider streams have emerged. One precursor G2 glider, not part of SGG1, is ejected first.

An alternative SGG1 generator consists of 4 gliders, which are shown about to collide (Fig. 13b0), consisting of 3 basic gliders, a G3 glider moving East, a G3 and G1 moving North West, and also a larger two-headed glider moving East. At time-step 14 the central rotating core of SGG1 has formed, plus 5 precursor gliders (3 G2, 2 G1), not part of SGG1, which are ejected first. After time-step 14 the six G1 gilder streams begin to emerge.

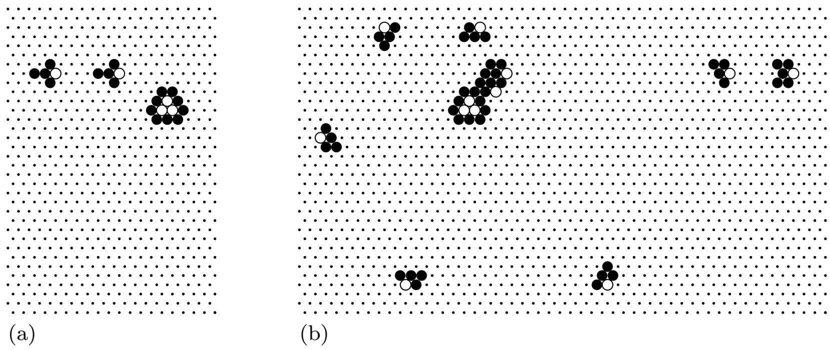

Figure 14: Creating a low-frequency spiral glider-gun SGG2. (a) Two G1 gliders approach the stationary localization SL1. (b) The spiral glider-gun SGG2 has formed, and the two G1 gliders have been transformed to G2 and G3.

The low-frequency spiral glider-gun SGG2 is created when two gliders interact with the stationary localization SL1. Fig. 14a shows a pair of G1 gliders moving West, one behind the other, and spaced 6 cells apart, about to brush past SL1 clockwise. The passing gliders perturb SL1 and transform it into a clockwise SGG2, shown in Fig. 14b. The pair of G1 gliders are changed to G2 and G3 gliders and continue traveling West. Remarkably, the stationary localization SL1 remains intact, but a satellite mobile localization is formed, which orbits SL1 and emits the 6 glider streams, with G2 gliders spaced 21 cells apart.

This scenario emerges naturally in spiral rule dynamics, because the spiral glider-gun SGG1 emits the precise glider stream required, G1 gliders with a 6 cell spacing, so SGG1 is responsible for the creation of SGG2. A steady stream of gliders from SGG1 brushing past the stationary localization SL1 at the right point will simply maintain the SGG2 dynamics.

The low-frequency spiral glider gun (SGG2) is somewhat vulnerable to attack by incoming gliders because of the wide spacing between ejected G2 gliders (21 cells), which can leave room for incoming gliders to penetrate and collide with the central satellite-localization. The SGG1 rotating center, on the other hand, is better protected by its high-frequency glider streams, and thus more stable. In the example in Fig. 15 we see a G2 glider, heading NE, approaching a SGG2

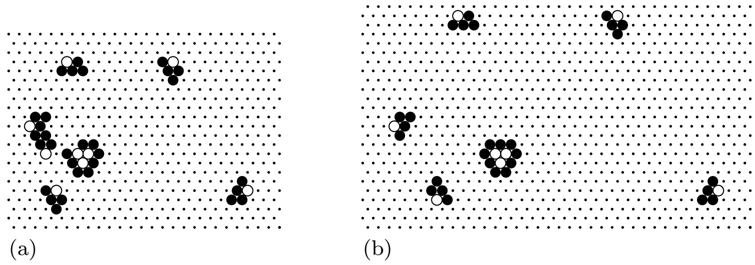

Figure 15: Destroying a low-frequency spiral glider-gun SGG2. (a) A G2 glider moving NE approaches the low-frequency glider-gun SGG2. (b) The gun is shut down leaving the stationary localization SL1 intact.

central satellite-localization orbiting anti-clockwise. The collision disrupts the satellite-localization, and SGG2 is transformed back to its original stationary localization SL1.

8 Mobile glider-guns

A mobile glider-gun is a localized traveling pattern with a complicated moving head, body and tail, which periodically emits or sheds streams of gliders in its wake, which move in various directions. Many types have been observed, emerging naturally in the evolution of the CA from random initial configurations, emitting one or more glider streams of basic gliders in various directions, and with various frequencies.

Some examples are shown in Fig. 16. In 16a just one stream of G3 gliders is emitted, moving in the opposite direction to the mobile glider-gun head, spaced at 8 cell intervals. In 16b two streams are emitted, G1 gliders with 16 cell spacing, and G2 gliders with 8 cell spacing. In 16c about 8 streams are emitted, depending on how they are counted, consisting of G1 and G2 gliders. Examples of glider-guns have been found emitting 3, 4, 5 and 6+ streams (not shown).

Mobile glider-guns are fragile structures because their unprotected heads can be easily destroyed when they collide head on with a stationary localization or with another glider.

9 Conclusion

We have constructed ternary cellular automata on a hexagonally tiled lattice which (i) simulates a inhibitor-activator (excitable) reaction-diffusion system, and (ii) supports the emergence of stationary generators of mobile localizations (spiral glider-guns), and stationary localizations, which together form complex circuits.

We described the commonly found emergent structures and their interactions, and how structures are created and annihilated. We have discovered

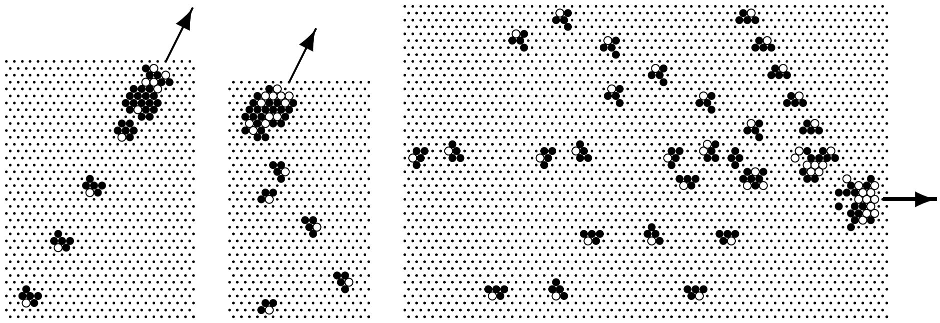

(a) (b) (c)

Figure 16: Mobile glider-guns: There are many types, consisting of a complicated moving head, body and tail, that sheds one or more gliders streams. In these examples the mobile glider-guns are moving in the directions indicated by the arrows.

several types of gliders: their collision outcomes include, reproduction, destruction, and stationary localizations. We showed that both gliders and stationary localizations can combine to form aggregations. We demonstrated that spiral glider-guns can emerge in glider collisions, and between gliders and static localizations, and may be destroyed if an incoming glider can penetrate to the central generator. We showed that spiral glider-guns can combine into compound glider-guns.

Also we demonstrated how streams of gliders emitted by spiral glider-guns can be controlled (switched and modified) with the help of stationary localizations that block or modify glider streams.

The dynamics are open ended. Structures can be positioned deliberately to see how they will interact, to create circuits with special properties. Many other types of structures that emerge spontaneously can be observed, but were not described in this paper. Given a large enough 2D lattice, we would expect to see a hierarchy of levels of emergent self-organization.

By interpreting transition rules in terms of quasi-chemical reactions, we proposed a theoretical framework for future implementations of the dynamics in chemical laboratory experiments. It would be absolutely unrealistic to claim at this stage of research that the quasi-chemical equations can be straightforwardly mapped onto real-life chemical systems. However, our previous experience in transforming "toy" cellular-automata models into real-life chemical prototypes (see e.g.[1]) tells us that it is just a matter of locating the appropriate chemical candidates and experimental conditions, although one would not expect to see any strong resemblance between chemical experimental implementations of the glider-gun and snapshots of the cellular-automata configurations. For example, the discrete topology of cellular-automaton lattices "keeps" mobile localizations (gliders) stable during indefinitely long periods of time, whereas wave-fragments — chemical analogs of gliders — in real chemical systems always either collapse or expand[1].

The spiral rule discussed in this paper, and related rules, may provide fruitful territory for designing sophisticated computational schemes, following the collision-based computing paradigm[2].

In forthcoming papers we will aim to uncover the computational potential of the spiral rule, and demonstrate how basic arithmetical operations can be implemented in cellular-automata which support gliders, stationary localizations, and spiral glider-guns.

References

[1] A. Adamatzky, B. De Lacy Costello, and T. Asai, *Reaction-Diffusion Computers* (Elsevier, 2005).

[2] A. Adamatzky (Ed.) *Collision-Based Computing* (Springer, 2003).

[3] A. Adamatzky, A. Wuensche, and B. De Lacy Costello, Glider-based computation in reaction-diffusion hexagonal cellular automata, Chaos, Solitons & Fractals 27 (2006) 287-295.

[4] M. Bär and L. Brusch, Breakup of spiral waves caused by radial dynamics: Eckhaus and finite wavenumber instabilities, New J. of Physics 6 (2004) 5.

[5] M. Bode, A. W. Liehr, C. P. Schenk and H. G. Purwins, Interaction of dissipative solitons: particle-like behaviour of localized structures in a three-component reaction-diffusion system. Physica D 161 (2000) 45-66.

[6] M. Gerhardt, H. Schuster and J. J. Tyson, A cellular excitable media. Physica D 46 (1990) 392415.

[7] H. Hartman and P. Tamayo, Reversible cellular automata and chemical turbulence, Physica D 45 (1990) 293-306.

[8] E. Bilotta, A. Lafusa and P. Pantano, Is self-replication an embedded characteristic of the artificial/living matter?, Artificial Life VIII, (MIT Press, 2003) 38-48.

[9] J. H. Conway, What is Life?, In: Winning ways for your mathematical plays, Chpt. 25, Vol.2, Eds. E. Berlekamp, J. H. Conway and R. Guy, (Academic Press, 1982).

[10] B. Chopard and M. Droz, *Cellular Automata Modeling of Physical Systems* (Cambridge University Press, 2005).

[11] G. Gáspár and K. Showalter, J. Am. Chem. Soc. 109, 4869 (1987).

[12] A. Ilachinski, *Cellular Automata: A Discrete Universe* (World Scientific, 2001).

[13] Q. Ouyang, H. L. Swinney and G. Li, Transition from spirals to defect-mediated turbulence driven by a doppler instability, Phys. Rev. Lett. 84 (2000) 1047-1050.

[14] I. Sediña-Nadal, E. Mihaliuk, J. Wang, W. Pérez-Muñuzuri and K. Showalter, Wave propagation in subexcitable media with periodically modulated excitability. Phys. Rev. Lett. 86 (2001) 1646.

[15] T. Toffoli and M. Margolus, *Cellular Automata Machines* (The MIT Press, 1987).

[16] J. R. Weimar, *Simulation with Cellular Automata* (Logos-Verlag, 1998).

[17] A. Wuensche, Classifying Cellular Automata Automatically, Complexity, 4 (1999) 47-66.

[18] A. Wuensche, *Discrete Dynamics Lab (DDLab)*, `www.ddlab.org`, 2005, also follow the links to "spiral-rule" and "self-reproduction".

[19] A. Wuensche, Glider dynamics in 3-value hexagonal cellular automata: The beehive rule, Int. J. of Unconventional Computing 1 (2005).

[20] S. Yaguma, K. Odagiri and K. Takatsuka, Coupled-cellular-automata study on stochastic and pattern-formation dynamics under spatiotemporal fluctuation of temperature. Physica D 197 (2004) 34-62.

[21] X. Yang, Computational modelling of nonlinear calcium waves, Appl. Mathem. Modelling, 30 (2006) 200-208.

[22] X. Yang, Pattern formation in enzyme inhibition and cooperativity with parallel cellular automata. Parallel Computing 30 (2004) 741-751.

[23] D. Young, A local activatorinhibitor model of vertebrate skin patterns. Math. Biosci. 72 (1984) 51.